Extraction of Si from Alkaline-Roasted Boron Ore Concentrate

Lv, Xiaoshu•; Ning, Zhiqiang; Zhai, Yuchun*+

School of Metallurgy, Northeastern University, Shenyang 110819, P.R. CHINA

Free, Michael

Department of Materials Science and Engineering, University of Utah, Salt Lake City, UT 84112, USA

Cui, Fuhui

School of Metallurgy and Environment, Central South University, Changsha 410083, P.R. CHINA

ABSTRACT: *The process of alkali roasting boron ore concentrate was proposed for the problems existing in the process of boron ore concentrate smelting. In this research, the influencing factors included the molar ratio of alkali to boron ore concentrate, roasting temperature, and roasting time were investigated. The single experiment and orthogonal experiments show the optimal conditions for roasting under the conditions evaluated including a temperature of 550°C, roasting time of 60 min, and a molar ratio of alkali to ore of 3:1. In the roasting process, the Si extraction correlated with the shrinking core model assuming a solid product layer according to XRD and SEM. Thus, the kinetics is controlled by diffusion through the product layer. The apparent activation energy for Si extraction was 13.47kJ/mol, and the roasting rate can be expressed as:* $1-(2/3\alpha)-(1-\alpha)^{2/3}=1.428\times10^{-2}\exp(-13470/RT)t$.

KEYWORDS: *Boron ore concentrate; Alkali roasting; Extraction; Kinetics.*

INTRODUCTION

Boron and its compounds are widely used in metallurgy, ceramics, permanent magnetic materials, Superconductor classification, whisker materials, and rare earth materials 00. Boron resources are abundant, but they are unevenly distributed around the world 0. Turkey has the largest reserves of boron deposits, accounting for about 70% of total boron reserves 0-00. China's reserves rank fourth in the world's boron reserves. The proven boron resources in China are mainly distributed in Liaoning, Qinghai, Tibet and Jilin. About 56% of them are in Liaoning Province. There are a lot of magnesium borate minerals in the Liaoning Boron Mine, the ore mineralization types are mainly szalbelyite and paigeite [0-0]. Szalbelyite (with an average of about 20% B_2O_3) is easy to process but is associated with relatively small reserves. At present, szalbelyite-based deposits, due to long-term mining, have been on the verge of depletion. Szalbelyite base resources are no longer sufficient 0.

***** *To whom correspondence should be addressed.*

+ E-mail: *zhaiyc@smm.neu.edu.cn*

● *Other Address: Liaoning Institute of Science and Technology, Benxi, 117000, P.R. CHINA*

1021-9986/2021/6/1999-2007 9/$/5.09

Table 1: Chemical Composition in boron ore concentrate (mass fraction, %).

Compositions	MgO	CO_2	SiO_2	Fe_2O_3	B_2O_3	Al_2O_3	CaO	Na_2O	other
content/%	36.40	5.38	32.30	9.89	8.92	2.56	1.77	0.11	2.51

Paigeite in Liaoning Province consists of mainly boromagnesite with large mineral reserves 0. It is a black ore body with iron, magnesium, and boron, which is difficult to separate 0-0. Boron-iron ore is associated with extensive resources, although this resource requires additional processing method development to enable effective resource recovery and utilization 00. Boron-magnesium ore (with an average of about 20% B_2O_3) is easy to process but has relatively small reserves. At present, Luanjiagou in Kuandian Manchu Autonomous County has the largest reserves of boron-magnesium ore in Wengquangou ore in Fengcheng, Liaoning Province, China, is mainly boromagnesite with large mineral reserves.

The boron ore concentrate often contains magnesium, iron, silicon, and boron. The smelting technology of boron ore concentrate is divided into pyrometallurgy and hydrometallurgy. Pyrometallurgy has the disadvantage of high energy consumption. The traditional hydrometallurgy methods include sulfuric acid leaching, soda leaching, ammonium sulfate leaching, and alkaline medium leaching 0-0. Sulfuric acid leaching is used in the wet process, but the corrosion of equipment by sulfuric acid has not been solved.

In this study, sodium hydroxide was used to roast boron ore concentrate (magnetically separated boron iron ore), SiO_2 was obtained by carbon separation in the dissolution solution, and borax was obtained by the effect of temperature of carbon separation solution on the solubility of borax. The dissolved slag was then leached by ammonium sulfate solution to obtain magnesium hydroxide and ferric hydroxide at different pH. This process enables the valuable elements in boron ore concentrate to be fully separated.

In this paper, boron ore concentrate was roasted with NaOH at selected temperatures. Silicon was extracted from ore concentrate following the roasting process. The effect of roasting time, roasting temperature, and the ratio of alkali to boron ore concentrate were investigated, and the kinetics in the roasting process was also investigated.

Boron iron ore and boron concentrate ore were obtained using Ludwigite Magnetic separation. In this research,

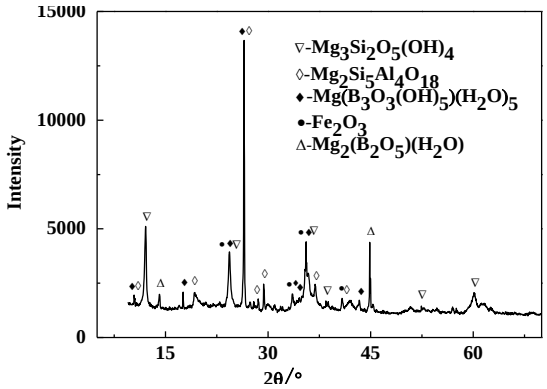

Fig. 1: XRD pattern of boron ore concentrate

boron ore concentrate was roasted with NaOH at selected temperatures. Silicon was extracted from ore concentrate following the roasting process. The effect of roasting time, roasting temperature, and the ratio of alkali to boron ore concentrate were investigated, and the kinetics in the roasting process was also investigated.

EXPERIMENTAL SECTION

Characterization of boron ore concentrate

The boron ore concentrate (liaoning shougang boron iron co. LTD.) in this roasting process was obtained from a mine in Dandong, Liaoning province, China. It was crushed and ground to a particle size less than 75 μm. Industrial NaOH was used as a reactant. The other regent used in the titration method was sourced from Sinopharm Chemical Regent Co., Ltd. (purity > 99.0%, AR).

The main contents detected by chemical methods in boron ore concentrate are listed in Table 1. The content of MgO is 36.40%, which is highest in boron ore concentrate. The contents of SiO_2, Fe_2O_3, and B_2O_3 are 32.30%, 9.89%, and 8.92% respectively.

XRD patterns of boron ore concentrate are presented in Fig. 1. The main mineral phases in boron ore concentrate are $Mg_3Si_2O_5(OH)_4$, $Mg_2Si_5Al_4O_{18}$, $Mg_2(B_2O_5)(H_2O)$, and $Mg_2B_3O_3\,(OH)_5\,(H_2O)_5$ as shown in Fig.1.

Fig. 2 (a) and (b) show the Scanning Electron Microscope (SEM) images of the boron ore concentrate. It can be seen that the particles have rough surfaces and

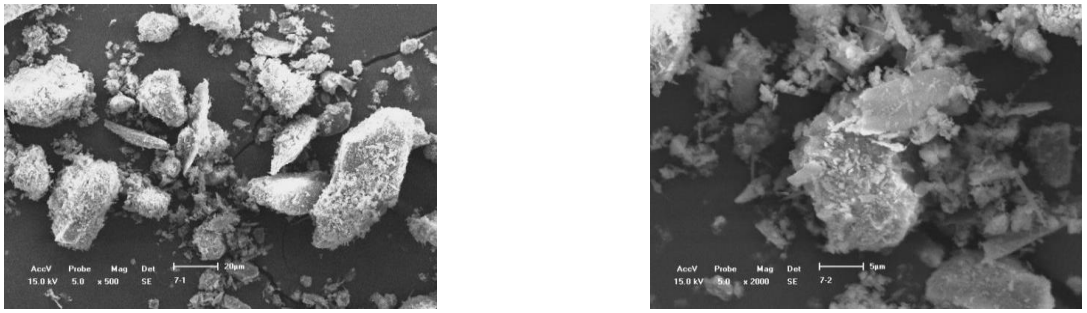

(a) (b)

Fig. 2: SEM images of the boron ore concentrate.

irregular in shapes. Most of the particles are relatively small, but there are still larger particles as shown in Fig. 2.

Procedures

The boron ore concentrate was grounded into fine powder in ball mill equipment (BS2308, TENCAN POWDER, and China) and dried at 105ºC for 8h, then mixed with alkali at a particular molar ratio in each experiment. The mixture was placed into a corundum crucible and put into a muffle furnace (Shanghai BenAng Scientific Instrument Co., Ltd., BA-2.5-10, Shanghai, China). The mixture was roasted at the same heating rate at different temperatures, when the heating stopped and the temperature of the system decreased below 150 °C, Afterwards, the roasted products were ground and leached with deionized water in a constant temperature water bath (DK-524-type, Changzhou Jintan Scientific Instrument Technology, Changzhou, China) at 95ºC for 30 min. The resultant liquor was leached, filtered using a vacuum filtration system, and the remaining solids were then washed twice with deionized water. The filtrate was analyzed to determine the concentration of silicon. The content of silicon in sodium silicate solution was determined by titration methods, and the silicon dioxide extraction rate was calculated as:

$$\alpha\left(SiO_2\right)=\frac{m'\left(SiO_2\right)}{m\left(SiO_2\right)}\times 100\% \quad (1)$$

Where $\alpha\,(SiO_2)$ is the extraction ratio of SiO_2, $m'(SiO_2)$ is the mass of SiO_2 in solution, and $m\,(SiO_2)$ is the mass of SiO_2 in boron ore concentrate.

Product Analysis

The content of elements in boron ore concentrate was determined by X-Ray Fluorescence analyzer (Xep03 STD Vakuum, Germany). The roasting products and residues were identified using a D/max RB X-Ray Diffraction instrument (Rigaku Corporation, D/max-RB, Tokyo, Japan) with Cu-Kα radiation ranging from 5~80° and a scanning speed of 10°/min. The analysis of the morphology of the roasted products was conducted using a Scanning Electron Microscope (Shimadzu, SSX-550, Tokyo, Japan). In the final leach liquor, the concentration of Si was measured by the sodium fluoride titration method [23].

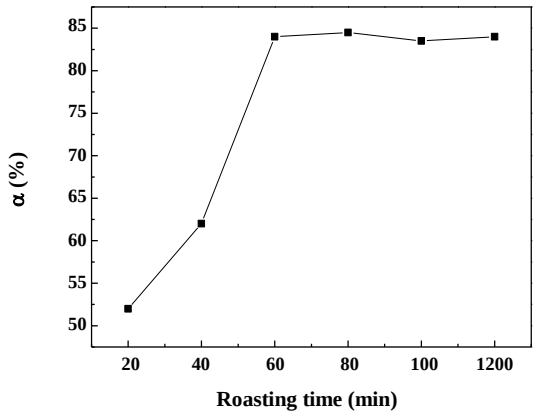

Fig.3: The effect of roasting time on the extraction.

RESULTS AND DISCUSSIONS

Effect of roasting time on the extraction of Si

The effect of roasting time on the extraction of Si as a function of time was studied using the roasting temperature of 550ºC and the molar ratio of alkali to ore of 3:1, and then the roasting products were leached at 95 ºC for 60min. The results are presented in Fig.3.

It can be seen from Fig.3 that the extraction increased gradually with in 60min, and then reached a plateau. The extraction reached 84% at 60min. This was mainly

Table 2: Results of orthogonal experiments.

No.	A(Temperature) /ºC	B(Molar ratio)	C(Time) / min	Recovery ratio / %
1	450	2:1	30	61.40
2	450	3:1	60	64.37
3	450	4:1	90	73.89
4	500	2:1	60	65.27
5	500	3:1	90	68.34
6	500	4:1	30	70.02
7	550	2:1	90	70.13
8	550	3:1	30	68.01
9	550	4:1	60	84.09
Average1	66.55	65.60	66.48	
Average2	67.88	76.91	71.24	
Average3	74.08	76.00	70.79	
R	7.53	10.40	4.78	$R_B>R_A>R_C$

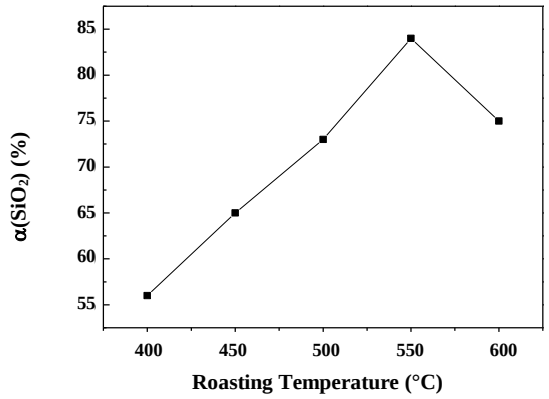

Fig.4: The effect of roasting temperature on the extraction.

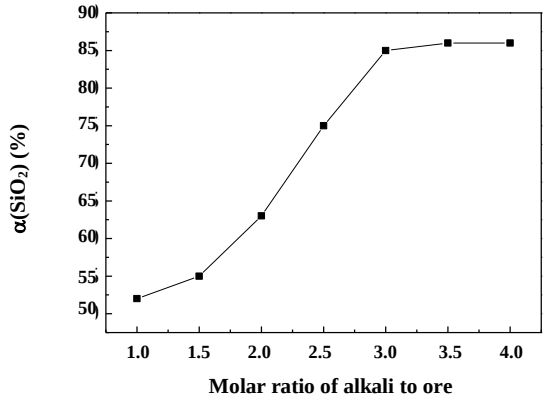

Fig.5: The effect of the molar ratio of alkali to ore on the extraction.

attributed to the formation of silicate in the roasting process. The extraction did not increase at times longer than 60 minutes.

Effect of roasting temperature on extraction of Si

The effect of roasting temperature in the range of 400-600 ºC on the extraction was investigated using the roasting time of 1h [24], the molar ratio of alkali to ore concentrate of 3:1, a leaching temperature of 95 ºC, and a leaching time of 60 min.

The results are presented in Fig.4. Fig.4 shows that roasting temperature has a significant effect on the extraction of SiO_2. The extractions of SiO_2 increased rapidly from the roasting temperature of 400 ºC (56%) to 550 ºC (84%). The decline result of the extraction of Si from 550 ºC to 600 ºC is the phase change at 575 ºC, which generates β-quartz that does not interact significantly with alkali.

Effect of molar ratio on the extraction of Si

Roasting at 550 ºC was applied in the following experiments. The effect of molar alkali on boron ore concentrate shows in Fig.5 in the condition of roasting time of 1h, the roasting temperature of 550 ºC, and leaching at 95 ºC for 60min.

Fig.8. shows that the extraction of silica increases with the molar ratio of alkali to ore from 1:1 to 3:1.

Orthogonal Design of Experiments

In order to obtain the optimal reaction condition of the roasting process, an orthogonal experiment was designed based on the single factor experiments on the extraction of Si. The orthogonal experimental results are shown in Table 2.

As shown in Table 2, the orthogonal experimental results show the effect of factors on the extraction as follows:

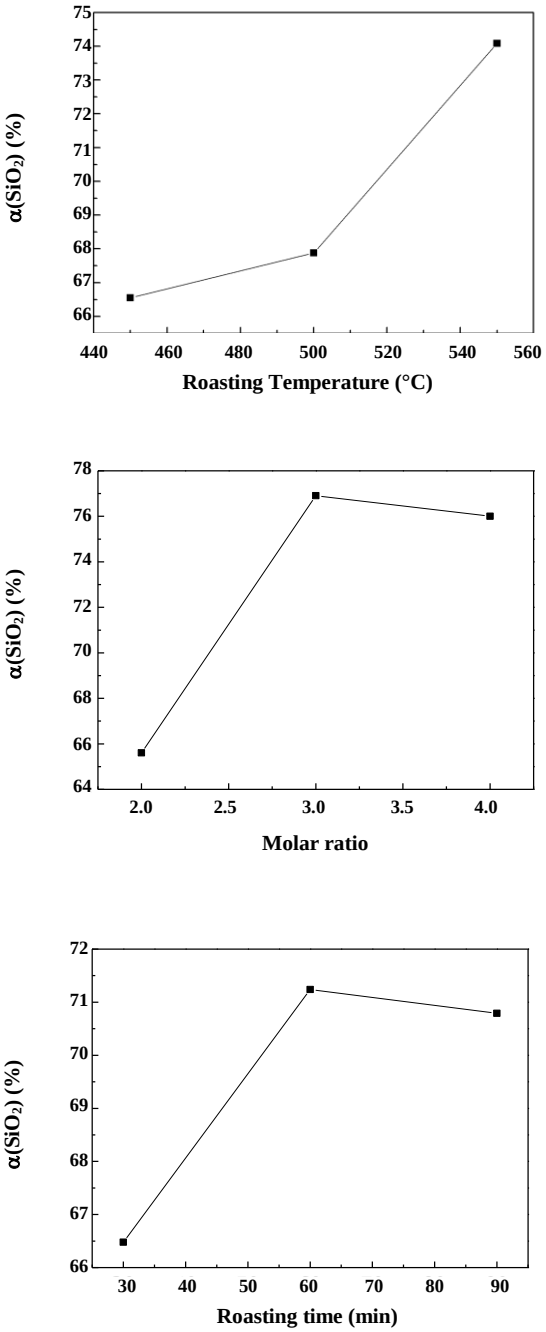

Fig.6: Tendency chart of range for the factors roasting temperature, the molar ratio of alkali to ore, and roasting time.

the molar ratio of alkali to ore, the roasting temperature, and roasting time. The trend of the range is shown in Fig.6. It can be seen that the optimum conditions of the The roasting process is the roasting temperature of 550 ºC, the molar ratio of alkali to ore of 3:1, and the roasting time of 60 min.

The Roasting Mechanism

To identify the roasting mechanism of mixed alkali with boron ore concentrate. The XRD analysis of clinkers was obtained by roasting ore samples with alkali at the temperature of 450ºC, 500 ºC, and 550 ºC as shown in Fig.7. The melting point of NaOH is 318 ºC. Therefore, the Alkali roasting ore reactions belong to liquid-solid reactions above 315 ºC.

At 450ºC, the new main phases of Na_2MgSiO_4, MgO, $Mg_2(B_2O_5)$, and $Na(Fe_{0.25}Al_{0.75})O_2$ were produced, while $Mg_3Si_2O_5(OH)_4$, $Mg_2Si_5Al_4O_{18}$, and $Mg_2B_3O_3(OH)_5(H_2O)_5$ in boron ore concentrate were gone, as shown in Eqs. (2- 6).

At 500 ºC, the new main phases of Na_2MgSiO_4, MgO, $Mg_2(B_2O_5)$, and $Na(Fe_{0.25}Al_{0.75})O_2$ were produced, while $Mg_3Si_2O_5(OH)_4$, $Mg_2Si_5Al_4O_{18}$, and $Mg_2B_3O_3(OH)_5(H_2O)_5$ in boron ore concentrate were gone, as shown in Eqs. (2-6). As the roasting temperature increased， phases ($Mg_2(B_2O_5)$, and $Na(Fe_{0.25}Al_{0.75})O_2$) were decomposed and new phases ($NaAlO_4$, $Na_2B_4O_7$, $NaFeO_2$) were generated as shown in Eqs. (7, 8).

$$M_3Si_2O_5(OH)_4 + 4NaOH \rightarrow 2Na_2MgSiO_4 + MgO + 4H_2O\uparrow \quad (2)$$

$$Mg_2Si_5Al_4O_{18} + 8NaOH \rightarrow 2Na_2MgSiO_4 + NaAlO4 + 3NaAlSiO_4 + 4H_2O\uparrow \quad (3)$$

$$2Mg(B_3O_3)(OH)_5(H_2O)_5 + 4MgO \rightarrow 3Mg_2(B_2O_5) + 15H_2O\uparrow \quad (4)$$

$$Mg_2(B_2O_5)(H_2O) \rightarrow Mg_2(B_2O_5) + H_2O\uparrow \quad (5)$$

$$Mg_2Si_5Al_4O_{18} + Fe_2O_3 + 16NaOH \rightarrow 4Na(Fe_{0.25}Al_{0.75}) + NaAlO_2 + 2MgO + 5Na2SiO_3 + 8H_2O\uparrow \quad (6)$$

$$4Na(Fe_{0.25}Al_{0.75})O_2 \rightarrow NaFeO_2 + 3NaAlO_2 \quad (7)$$

$$2Mg_2(B_2O_5) + 2NaOH \rightarrow Na_2B_4O_7 + 4MgO + H_2O\uparrow \quad (8)$$

Kinetic analysis

The process of roasting boron ore concentrate with NaOH is a typical liquid-solid reaction the shrinking core

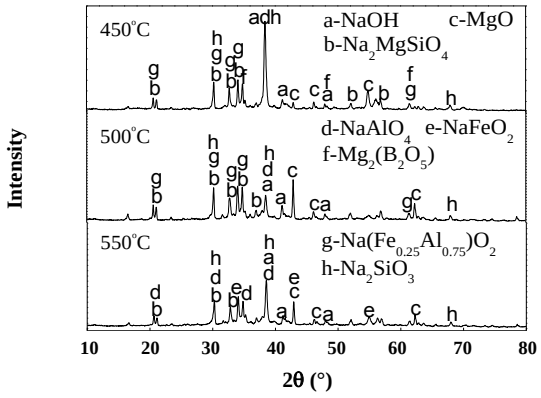

Fig.7: XRD patterns at different roasting temperatures for 60 min and alkali to ore ratio 3:1.

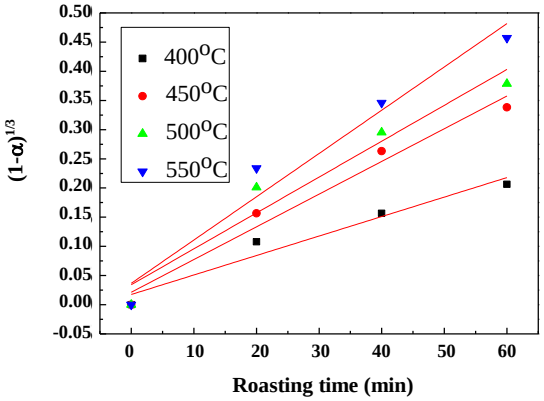

Fig. 9: Plot of 1-(1-α)$^{1/3}$against roasting time at different roasting temperatures

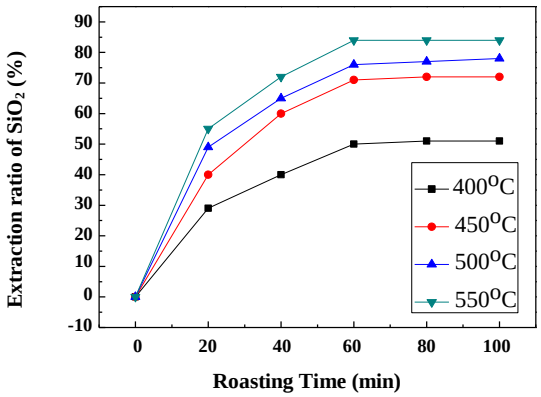

Fig.8: Effect of roasting temperature on the extraction.

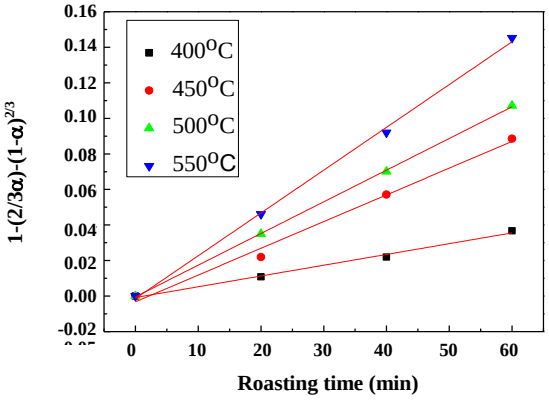

Fig. 10: Plot of 1-(2/3α)-(1-α)$^{2/3}$against roasting time at different roasting temperatures.

model is the common kinetic model for this type of reaction. The reaction between the silicon in the ore and NaOH products soluble sodium silicate, and insoluble solid products (Na_2MgSiO_4, MgO, and $NaFeO_2$), and generated a layer of insoluble solid products on the particle surface, which can be analyzed with the shrinking core model [26]. For this model, the reaction rate between solid particles and reaction reagents may be controlled by one of the following steps: diffusion through the liquid film, diffusion through the product layer, or the chemical reactions at the surface. The following expression can be used to describe the kinetics of the roasting process if the surface chemical reaction is the rate-controlled step [27-28]:

$$1-(1-\alpha)^{1/3} = k_c t \qquad (9)$$

However, if the alkali roasting reaction rate is controlled by the diffusion through a solid product layer, the following expressed of the shrinking core model can be appropriate to describe as:

$$1-(2/3)\alpha-(1-\alpha)^{2/3} = k_d t \qquad (10)$$

Where t is reaction time (min), α is the extraction of silica, and k_c and k_d are reaction rate constants.

The effect of roasting temperature on the extraction ratio of Si was investigated from 400 °C to 550 °C at a molar ratio of alkali to ore of 3:1 as shown in Fig.8.

The extraction increased with a roasting temperature rising in Fig.8. According to the shrinking core model. The experimental data presented in Fig. 8 were fitted with Eq. (9) and Eq. (10), and the results are shown in Figs. 9 and 10. The rate constants and their correlation coefficients were given in Table 3 for the surface chemical reaction and

Table 3: The apparent rate constant-coefficient values at the different reaction temperatures.

Reaction temperature(°C)	$1-(1-\alpha)^{1/3}$		$1-(2/3)\alpha-(1-\alpha)^{2/3}$	
	k_r (min^{-1})	R^2	k_d (min^{-1})	R^2
400	0.00334	0.9608	6.0635×10^{-4}	0.9910
450	0.0056	0.9259	0.015	0.9879
500	0.00615	0.9414	0.0178	0.9997
550	0.00742	0.9339	0.0241	0.9970

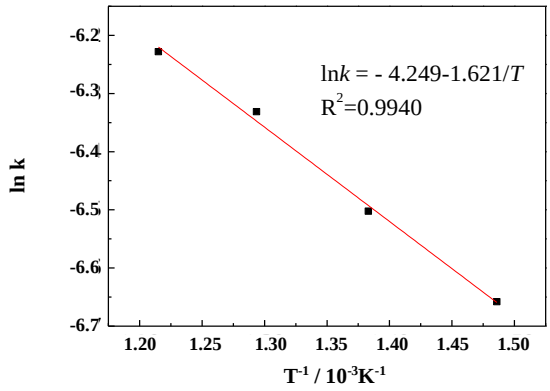

Fig. 11: Plot of lnk against 1/T.

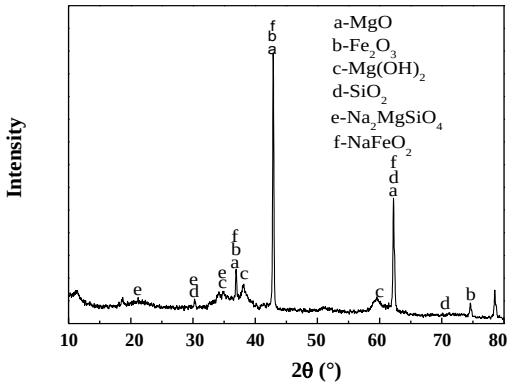

Fig. 12: XRD pattern of the leaching residue.

the diffusion-controlled model. There is no good linear relation between $1-(1-\alpha)^{1/3}$ and roasting time, which the linear relationship between $1-(2/3\alpha)-(1-\alpha)^{2/3}$ and roasting time. So it was determined that the experimental date fit better with the model of $1-(2/3\alpha)-(1-\alpha)^{2/3}=k_dt$.

It is generally accepted that the diffusion-controlled model was suitable for this roasting process.

The Arrhenius equation can be represented in modified form as [29]:

$$k = A\exp(-E/RT) \quad (11)$$

Where A is the pre-exponential factor (time^{-1}), E is apparent activation energy (J.mol), and R is gas constant (J/mol^{-}K), T is Thermodynamic temperature (K).

According to the Arrhenius law shown in Eq. (11), the plot of ln$k$ against 1/T is shown in Fig.11. The results of apparent activation energy and pre-exponential factor are calculated from the slope and intercept of the Arrhenius plot in Fig.11, and the values are 13.47 kJ/mol and 1.428×10^{-2}min^{-1}. Apparent activation energy is less than 20kJ/mol, it belongs to the shrink nucleus model controlled by diffusion, which is consistent with the conclusion of the figure. Thus, the roasting process kinetics equation can be expressed as

$$1-(2/3)\alpha-(1-\alpha)^{2/3} = 1.428\times10^{-2}\exp(-13470/RT)t \quad (12)$$

Characterization of residue after silicon extraction

The leaching residue was obtained by alkali roasted boron ore concentrate under the conditions that the roasting temperature of 550°C, the roasting time of 60min, and the molar ratio of alkali to ore of 3:1, washed to neutral, Fig. 10 and Table 3.

The XRD pattern and the SEM image of the leaching residue are shown in Fig.12 and Fig.13. The main phases in the residue are magnesium oxide, iron oxides, $Mg(OH)_2$, quartz silica, $NaFeO_2$, and Na_2MgSiO_2. The leaching residue presents fluffy bulbous that reunites together.

CONCLUSIONS

In conclusion, the effects of roasting temperature, roasting time, and the molar ratio of alkali to ore on the extraction in alkali roasting boron ore concentrate

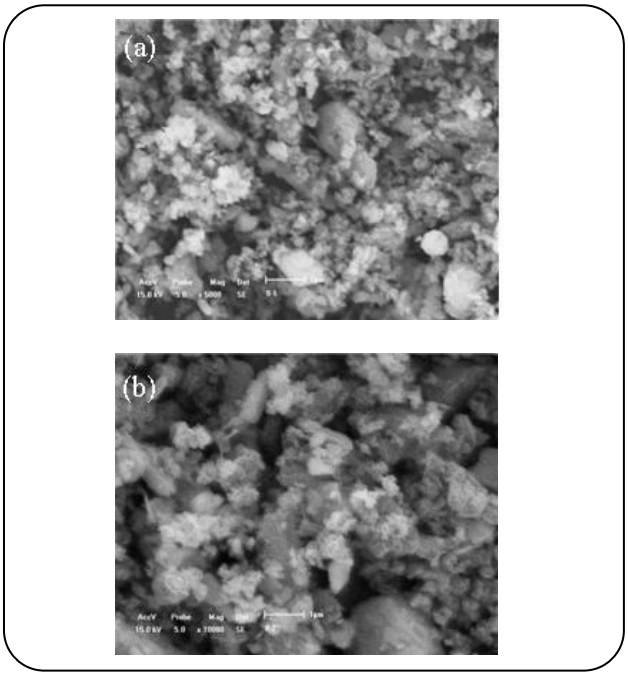

Fig. 13: SEM image of leaching residue.

were investigated. Orthogonal experiments were carried out on the basis of single-factor experiments. The results showed that the extraction could be improved by increasing the roasting temperature, roasting time, and the molar ratio of alkali to ore. The optimum roasting conditions using alkali roasting boron ore concentrate are that the roasting temperature is 550°C, the roasting time is 60 min, and the molar ratio of alkali to ore is 3:1. Under the best experimental conditions, the extraction can be reached more than 84%. The alkali roasting boron ore concentrate kinetics was studied, which was found to obey the shrinking core model for the diffusion-controlled. The activation energy was determined to be 13.47kJ/mol, and the kinetics model equation is expressed as:

$$1-(2/3\alpha)-(1-\alpha)^{2/3}=1.428\times10^{-2}\exp(-13470/RT)t$$

Acknowledgments

This work was funded by the Natural Science Foundation of China, grant number 41701300, Scientific Research Foundation of Liaoning Province, grant number 201601338.

Received : Apr. 17, 2020 ; Accepted : Jul. 20, 2020

REFERENCES

[1] Sun Qing, Zheng Shui-lin, Li Hui, Hou Hui-li. Boron Resource and Prospects of Comprehensive Utilization of Boron Mud as a Resource in China, *Earth Science Frontiers*, **21(5)**: 325–330 (2014).

[2] Jiang S.Y., Boron Isotope Geochemistry of Hydrothermal ore Deposits in China: A Preliminary Study, *Physics and Chemistry of the Earth Part A Solid*, **26**: 851–858 (2001).

[3] Yakup Kar, Nejdet Şen, Ayhan Demirbaş. Boron Minerals in Turkey, Their Application Areas and Importance for the Country's Economy, *Minerals and Energy-Raw Materials Report*, **20(2)**: 2–10 (2006).

[4] Tang Yao, Chen Chun-lin, Xiong Xian-xiao, Gao Peng. World Boron Distribution and Current Status of Its Exploitation and Development, *Modern Chemical Industry*, **33(10)**: 1−4, 6 (2013). (in Chinese)

[5] Ning Zhi-Qiang, Song Qiu-shi, Zhai Yu-Chun, Xie Hong-Wei, Yu Kai. Desilication Kinetics of Calcined Boron Mud in Molten Sodium Hydroxide Media, *Journal of Central South University*, **23**: 2191−2198 (2016).

[6] Li G., Liang B., Rao M., Zhang Y., Jiang T., An Innovative Process for Extracting Boron and Simultaneous Recovering Metallic Iron from Ludwigite Ore, *Miner. Eng.*, **56**: 57–60 (2014).

[7] Qiao X., Li W., Zhang L., White N.C., Zhang F., Yao Z., Chemical and Boron Isotope Compositions of Tourmaline in the Hadamiao Porphyry Gold Deposit, Inner Mongolia, China. *Chemical Geology*, **519**: 39-55 (2019).

[8] Gemici Unsal, Tarcan Gultekin, Helvac Cahit, Somay A. Melis, High Arsenic and Boronconcentrations in Groundwaters Related to Mining Activity in the Bigadic Borate Deposits (Westernturkey), *Applied Geochemistry*, **23(8)**: 2402-2407 (2008).

[9] Zhong Hu-Rui, Wen Qi-Hua, Fu Zhou-Mei, Su Wen-Chao, Wu Bi-Xian, Tang Peng-Jian, Zhong Hong. Geological and Geochemical Constraints on the Origin of the Giant Lincang Coal Seamhostedgermanium Deposit, Yunnan, SW China: A Review, *Ore Geology Reviews*, **36(1-3)**: 221-234 (2009).

[10] Ning Zhi-Qiang, Zhai Yu-Chun, Zhou Di, Cao Yong-xin, Gu Hui-min. Study of the Technique for the Preparation of Epsosmalt from the Boron Mud, *Light Metal*, 2007(7): 61−63. [in Chinese]

[11] Lv X., Cui F., Ning Z, Free M.L., Zhai, Yuchun, Mechanism and Kinetics of Ammonium Sulfate Roasting of Boron-Bearing Iron Tailings for Enhanced Metal Extraction, *Processes*, **7(11)**: 812 (2019).

[12] Guliyev R., Kuşlu S., Çalban T., Çolak S., Leaching Kinetics of Colemanite in Potassium Hydrogen Sulphate Solutions, *Journal of Industrial and Engineering Chemistry*, **18(1)**: 3844 (2012).

[13] DING Y., Wang J., Wang G., MA S., Xue Q., Comprehensive Utilization of Paigeite Ore Using Iron Nugget Making Process, *Journal of Iron and Steel Research International*, **19(6)**: 9-13 (2012).

[14] Jie L., Fan Z.G., Liu Y.L., Liu S.L., Jiang T., Xi Z.P., Preparation of Boric Acid from Low-Grade Ascharite and Recovery of Magnesium Sulfate, *Tran. Nonferrous Met. Soc. China*, **20**: 1161–1165 (2010).

[15] Yang T., Dou A., Lei C., Ren J., Liu Z., Ligand Selection for Complex- Leaching Valuable Metals in Hydrometallurgy, *Transaction of Nonferrous Metals Society of China*, **20(6)**: 1148-1153 (2010).

[16] Guliyev R., Ku¸slu S., Çalban T., Çolak S., Leaching Kinetics of Colemanite in Potassium Hydrogen Sulphate Solutions, *J. Ind. Eng. Chem.*, **18**: 38–44 (2012).

[17] Liang B., Li G., Rao M., Peng Z., Zhang Y., Jiang T., Water Leaching of Boron from Soda-Ash-Activated Ludwigite Ore, *Hydrometallurgy*, **167**: 101–106 (2017).

[18] Erdo ˘Gan Y., Aksu M., Demirba¸s A., Abalı Y., Analyses of Boronic Ores and Sludges and Solubilities of Boron Minerals in CO_2-Saturated Water, *Resour, Conserve Recycle*, **24**: 275–283 (1998).

[19] Kavcı E., Calban T., Colak S., Ku¸slu S., Leaching Kinetics of Ulexite in Sodium Hydrogen Sulphate Solutions, *J. Ind. Eng. Chem.*, **20**: 2625–2631 (2014).

[20] Qin S., Yin B., Zhang Y., Zhang Y., Leaching Kinetics of Szaibelyite Ore in NaOH Solution, *Hydrometallurgy*, **157**: 333–339 (2015).

[21] Xu Y., Jiang T., Zhou M., Wen J., Chen W., Xue X., Effects of Mechanical Activation on Physicochemical Properties and Alkaline Leaching of Boron Concentrate, *Hydrometallurgy*, **173**: 32–42 (2017).

[22] Xu Y., Jiang T., Wen J., Gao H., Wang J., Xue X., Leaching Kinetics of Mechanically Activated Boron Concentrate in a NaOH Solution, *Hydrometallurgy*, **179**: 60–72 (2018).

[35] Maghsoudi P., Sadeghi S., Xiong Q., Aminossadati S.M., A Multi-Factor Methodology for Evaluation and Optimization of Plate-Fin Recuperators for Micro Gas Turbine Applications Considering Payback Period as Universal Objective Function, *International Journal of Numerical Methods for Heat & Fluid Flow*, **30(5)**: 2411-2438 (2019).

[36] Towler G., Sinnott R., "Chemical Engineering Design: Principles, Practice and Economics of Plant and Process Design", 2nd ed, Capital Cost Estimating, *United Kingdom: Butterworth-Heinemann*, (2013).

[37] Chemical Engineering Essential for The CPI Professional, *Chemical Engineering Plant Cost Index*, https://www.chemengonline.com/2019-cepci-updates-january-prelim-and-december-2018-final/2018/ (Accessed 10 September 2019).

[38] U.S. Energy Information Administration (eia), *Electric Power Monthly*, https://www.eia.gov/electricity/monthly/, December 2018 (Accessed 6 September 2019).

[39] U.S. Energy Information Administration (eia), *Price of Liquefied Natural Gas Exports*, https://www.eia.gov/dnav/ng/hist/n9133us3M.htm, October 2018 (Accessed 6 September 2019).

[40] Maghsoudi P., Sadeghi S., A Novel Economic Analysis And Multi-Objective Optimization of a 200-kW Recuperated Micro Gas Turbine Considering Cycle Thermal Efficiency and Discounted Payback Period, *Applied Thermal Engineering*, **166**:114644 (2020).

[41] Hanafizadeh P., Maghsoudi P., Exergy, Economy and Pressure Drop Analyses for Optimal Design of Recuperator Used in Microturbine, *Energy Equipment and Systems*, **5(2)**: 95-113 (2017).